Research Article Vol. 7, No. 12 / December 2020 / Optica 1781

Unraveling the origin of frequency modulated combs using active cavity mean-field theory

David Burghoff

Department of Electrical Engineering, University of Notre Dame, Notre Dame, Indiana 46656, USA (dburghoff@nd.edu)

Received 2 September 2020; revised 21 October 2020; accepted 5 November 2020 (Doc. ID 408917); published 14 December 2020

In many laser systems, frequency combs whose output is frequency-modulated (FM) can form, producing light whose frequency sweeps linearly. While this intriguing result has been replicated experimentally and numerically, a compact description of the core physics has remained elusive. By creating a mean-field theory for active cavities analogous to the Lugiato–Lefever equation, we show that these lasers are described by a nonlinear Schrödinger equation with a potential proportional to the phase of the electric field. This equation can be solved analytically and produces a field with quasi-constant intensity and piecewise quadratic phase. We refer to these nondispersive waves as *extendons*, and they describe both fundamental FM combs and harmonic states. Our results apply to many lasers, explaining the ubiquity of this phenomenon, and our new theory unifies many experimental observations.

https://doi.org/10.1364/OPTICA.408917

1. INTRODUCTION

Frequency-modulated (FM) combs are a type of frequency comb that have been produced in a number of laser systems. First observed decades ago in electro-optically modulated cavities [1], such lasers were known to not produce pulses but would instead produce an FM output [2]. These systems were assumed to have sinusoidal modulation based on their spectra, but no direct measurements of the temporal output could be performed since the peak intensities were too low. More recently, it has been shown that many lasers spontaneously enter self-FM regimes, where the FM is produced without any external modulation and the amplitude is approximately constant. This effect has been seen primarily in semiconductor lasers: in quantum cascade lasers (QCLs) [3–6], quantum dot lasers [7], diode lasers [8,9], etc. While not pulses, these combs can still be used in applications such as dual-comb spectroscopy [10–12]. They are distinct from Fourier domain mode-locked lasers [13] in that these combs generate their own frequency modulation, instead of having a frequency sweep that is externally applied.

Earlier FM comb observations relied only on observations of a narrow coherent beatnote and of a broadband spectrum. However, it is well known that these observations are not sufficient to fully reconstruct the temporal profile. Indeed, early reports of pulse formation in QCLs were later determined to have had quasi-constant intensities [14]. It was only recently, with the development of Shifted Wave Interference Fourier Transform Spectroscopy (SWIFTS) [15–17], that it became possible to measure high-quality temporal traces of low-intensity combs. Surprisingly, it was found that many of these FM combs do not have sinusoidal modulation; they have linear-chirped operation [6–8,17] (or boxcar operation when the gain spectrum is discontinuous [16]). This chirp is completely coherent and comprises the whole laser spectrum [18,19]. It can also manifest as harmonic states, where the FM behavior repeats an integer number of times per round trip [20].

While linear-chirped behavior is a robust result that has been replicated in many different systems, it is not fully understood. Primarily, these systems are simulated using Maxwell–Bloch formalisms, which lead to a series of eight coupled partial differential equations [21–26]. Alternatively, they can be simulated using modal expansions of optical nonlinearities [4,20,27,28] or a coupled master equation description [29,30]. All of these results can reproduce FM comb formation, but as numerical descriptions they do not fully explain why the phenomenon appears in so many different systems. In addition, most of these results require the integration of many small time steps, making rigorous investigation more difficult. Still, the emergence of linear FM operation is apparently ubiquitous and robust, which suggests that a deeper mechanism is at play. Gaining a fundamental understanding of this behavior would be critical for improving the performance of FM combs and for discovering new states of light.

In this work, we show that all of these FM comb states are described by a single underlying phenomenon: the generation of nonlinear phase potentials. Above threshold, nearly any laser with substantial mirror losses can have its electric field described by a nonlinear Schrödinger equation (NLSE) with a potential proportional to its phase:

$$-i\frac{\partial F}{\partial T}=\frac{\beta}{2}\frac{\partial^2 F}{\partial z^2}+\gamma|F|^2(\arg F-\langle\arg F\rangle)F+ir(|F|^2-P_0)F, \tag{1}$$

where F is the electric field normalized to the unitless intracavity gain (proportional to the laser's steady-state intracavity intensity), T is the slow time, β is the normalized group velocity dispersion (GVD), γ is the nonlinear cross-steepening, angle brackets represent an average over position, and r represents amplitude relaxation to the steady state intensity at the left facet, P_0. Note that the position z is within the artificially extended laser cavity: if L_c is the physical cavity length, waves traveling in the positive direction are mapped to $z \in [0, L_c)$, waves traveling in the negative direction are mapped to $z \in [-L_c, 0)$, and periodic boundary conditions are used. Unlike the conventional NLSE, whose potential famously depends on the *intensity* of the electric field, here it is primarily determined by its *phase*. The fundamental solution to this equation can be written analytically as

$$F(z, T) = A_0 \exp\left[i\frac{\gamma|A_0|^2}{2\beta}\left(z^2 - \frac{1}{3}L_c^2\gamma|A_0|^2 T\right)\right], \quad (2)$$

where $A_0 = \sqrt{P_0}(1 + \frac{\gamma}{2r})^{-1/2} \approx \sqrt{P_0}$ is the wave's amplitude. Equation (2) can be considered the fundamental FM comb. Its phase is piecewise quadratic, leading to a linear chirp, and at the boundary its derivative is undefined. Like the celebrated sech^2 solitons that result from an intensity potential, this solution is nonperturbative and can be used as a starting point for more sophisticated analysis. It is dissipative and nondispersive, and does not change shape as it propagates. Unlike cavity solitons, it is inherently *delocalized* and must extend a full round trip to remain stable. In analogy to solitons, we refer to these nondispersive extended waves as *extendons*.

We will show that this result can be used to understand all of the salient features of FM combs that have been experimentally and numerically observed. For example, this result explains the pulsation that is frequently observed at the turnaround point where the frequency abruptly changes. It explains why these structures are not observed in other nonlinear media with self-steepening, such as microresonators and fibers. It explains why they do not form in ring cavities, which instead support lower-bandwidth states governed by a Ginzburg–Landau equation [30–32]. It also predicts the existence of harmonic states—analogous to higher-order solitons—and it allows us to analytically examine the conditions under which FM combs can form.

To arrive at this result, we must first develop a new mean-field formalism that describes the propagation of light in nonlinear laser cavities and shows how these phase potentials are produced. It is analogous to the celebrated Lugiato–Lefever equation (LLE) used to describe many nonlinear resonators, such as fiber ring resonators [33,34], microresonator Kerr combs [35–40], and Fabry–Perot (FP) [41–43] Kerr combs. The realization that the LLE was an excellent description of Kerr combs marked a turning point in their development, allowing them to be understood at a deep level [44,45]. FM combs have lacked such a description until now. We use the concept of the extended-cavity theory that has been used to describe the dynamics of nonlinear FP cavities [42,46], but with a key difference—we take into account the large changes of the field that are present in a laser cavity with substantial mirror losses and spatially varying gain. Though the resulting equation is integral, it greatly simplifies analysis and reproduces essentially all experimental data, reducing to the NLSE with some weak assumptions. We anticipate that it will be useful for the creation of novel FM comb states, just as the LLE has proven useful at predicting soliton states in Kerr combs and other novel states such as dark solitons [47], Turing rolls [40,48,49], soliton crystals [40,50,51], etc. We will show how phase potentials arise naturally from the cross-steepening nonlinearity, suggesting ways they can be engineered.

2. RESULTS

To show how lasers naturally give rise to the NLSE with a phase potential, we first derive a mean-field equation that describes the propagation of light within lasers with large spatial hole burning and mirror losses. Mean-field theory is a powerful technique that allows for the dynamics of nonlinear resonators to be evaluated over timesteps much larger than would otherwise be required, even multiple round trips. For example, the LLE has been critical for the understanding of Kerr combs [35], and can be modified for FP cavities [42,46]. Unfortunately, lasers with large internal gain and losses have not been described in this way, as large internal effects make averaging difficult. Even though the changes in the field after a *complete* round trip are typically small, the changes in the field *within* a round trip can be quite large. For example, lasers with large mirror losses experience exponential gain inside the cavity and delta function loss at the mirrors. To address this challenge, we normalize the electric field of the cavity to its steady state intensity, defining the envelope $F(z, t)$ as $E(z, t) \equiv K^{1/2}(z)F(z, t)$. Here $K \equiv P/P_0$ is a spatially varying gain function proportional to the laser's steady-state power in the absence of any phase-coupling terms, i.e., without dispersion and nonlinearity. The full derivation is given in Supplement 1, and in terms of normalized parameters the result is that

$$\frac{\partial F}{\partial T} = i\frac{1}{2}\beta\frac{\partial^2 F}{\partial z^2} + \frac{1}{4}D_g\frac{\partial^2 F}{\partial z^2} - \tilde{K}\left[\gamma_1\frac{\partial F^*}{\partial z}F + \gamma_2 F^*\frac{\partial F}{\partial z}\right]F - \frac{1}{3}r\left(|F|^2 + 2\langle K\rangle^{-1}\tilde{K}[|F|^2] - 3P_0\right)F, \quad (3)$$

where T denotes slow time, β represents dispersion, D_g represents gain curvature, r represents energy relaxation, and γ_1 and γ_2 represent cross-steepening. Cross-steepening is the primary nonlinear process responsible for FM comb generation. It is similar to the self-steepening that occurs in fibers [52], and can be construed as being related to an intensity-dependent group velocity. In a laser, it arises directly from the gain medium. In contrast to self-steepening, cross-steepening arises from the intensity of the counterpropagating wave. Here we also have defined $\tilde{K}[f](z)$ as a convolution between K and the arbitrary function f; these convolutions arose because the cavity contains forward and backward propagating waves. In comparison with the standard LLE and the FP-LLE formalisms derived for propagation within low-loss cavities [42,45,53], this formalism is somewhat more complicated due to the presence of the convolutions involving K. Still, this is essential for understanding FM comb operation, as it is the spatial dependence of K that gives rise to stable FM comb formation. Though this equation is integral in nature, it is highly amenable to numerical analysis since it is convolutional and can be rapidly evaluated using Fourier methods. It is readily solved using split-step methods, as is commonly done in fibers and other nonlinear resonators.

This formalism is readily extendable to more complicated gain spectra, and explains temporal traces observed in the terahertz [16] and in the mid-infrared (mid-IR) [54] (Fig. 1). For a mid-IR QCL with a gain spectrum well approximated by a Lorentzian, linearly chirped behavior is produced. However, if the

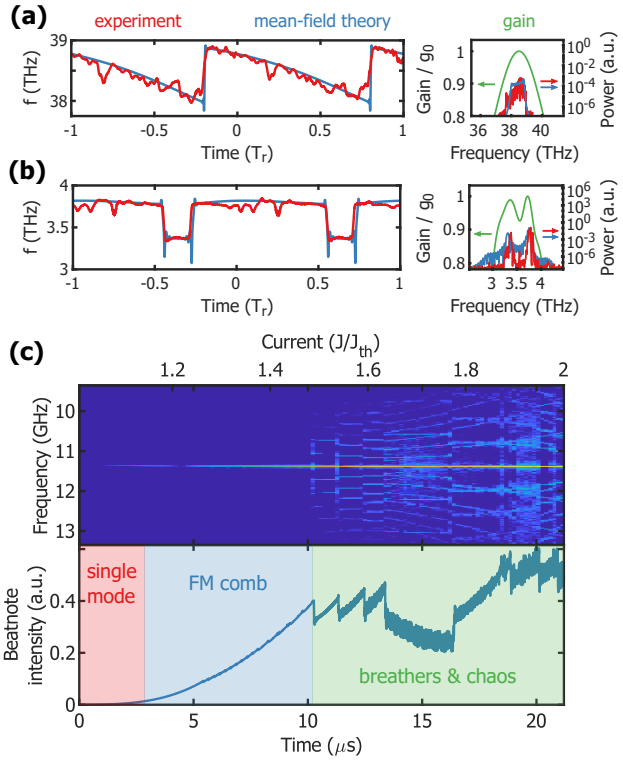

Fig. 1. (a) SWIFTS trace and mean-field theory description of a mid-IR QCL comb. The spectrum is linearly chirped since the gain spectrum is continuous. The gain and power spectra are also shown. (b) SWIFTS trace and mean-field theory description of a THz QCL with a double-peaked lineshape. When the experimentally measured lineshape is put into the model, the boxcar modulation is correctly reproduced. (c) Simulated beatnote map of a mid-IR QCL comb above threshold (GVD of $-2500\ \mathrm{fs}^2/\mathrm{mm}$) as the current is ramped over 250,000 round trips. The laser is initially single mode, then enters an FM comb regime, then enters a high phase noise regime dominated by breathers and chaos. Similar behavior has been observed in numerous comb systems [56–58].

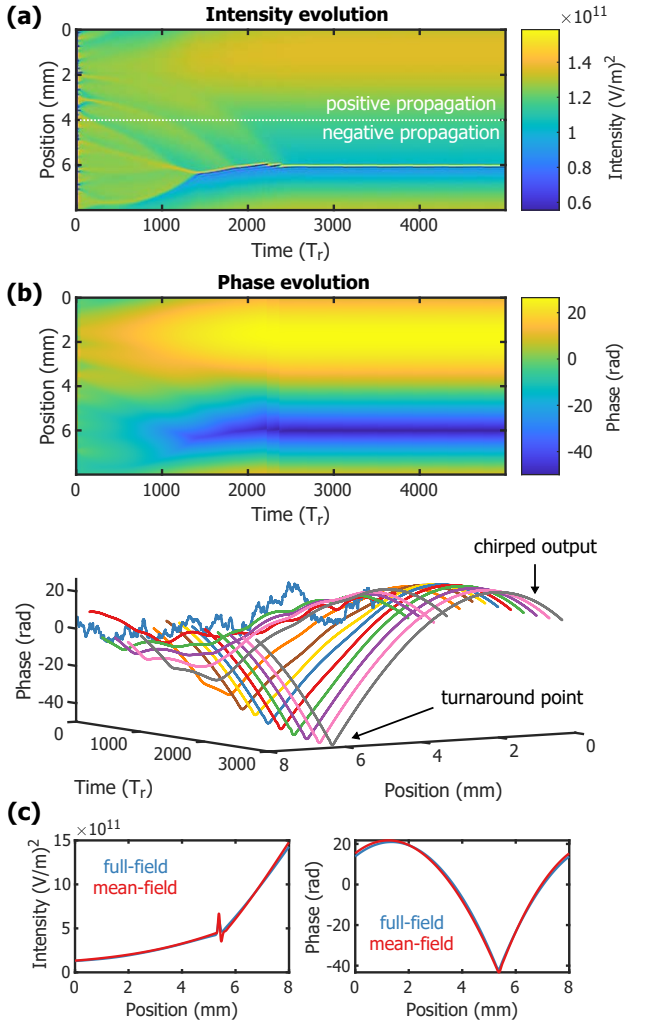

Fig. 2. Split step simulation of a QCL using the mean-field theory described by Eq. (3). Parameters are given in Supplement 1, Table 1, and the QCL has a GVD of $-2000\ \mathrm{fs}^2/\mathrm{mm}$ and zero Kerr nonlinearity. Position values below $L_c = 4$ mm represent positive propagation; values above L_c represent negative propagation. (a) Evolution of the normalized intracavity intensity over 5000 round trips. The intensity quickly builds to a constant value from spontaneous emission, then gains minor modulation due to comb formation. (b) Evolution of the phase. The phase begins random, and eventually gives way to a periodic parabola with an abrupt turnaround point. (c) Comparison of the full-field simulation [Eq. (S1)] to the mean-field simulation [Eq. (3)].

gain spectrum is double-peaked, as was the case for the terahertz temporal traces in Ref. [16], then the comb spectrum breaks into sub-combs. Temporally, this results in a switching behavior, with a trace resembling a boxcar modulation. Describing this effect requires that the gain curvature term be replaced by the medium's actual lineshape function, but this is naturally implemented using split-step methods. When the experimental lineshape measured by terahertz time domain spectroscopy [5] is used as an input to the mean-field model, the boxcar modulation is correctly reproduced. Likewise, this model correctly produces the beatnote maps that are commonly observed experimentally; for moderate dispersion values, a laser will have a single-mode regime at low pumps, an FM comb regime at moderate pumps, and a chaotic regime at large pumps.

An example of simulating a typical mid-IR QCL comb with a split-step implementation of the mean-field theory is shown in Fig. 2. The field is initialized to a low value and initially stabilizes to its steady-state intensity. Over many round trips, the phase builds and eventually gives way to a periodic parabola, representing an FM comb (whose frequency is linearly chirped). Because we need only take one time step per round trip, the simulation takes only seconds and agrees with the full-field theory. In addition, as the mean-field theory has been constructed in a way that removes the wave's explicit dependence on position, one can alternatively treat the position variable as a co-moving coordinate. This allows for timesteps to be taken that are fractions of a round trip (for additional accuracy) or multiples of a round trip (for additional speed). Note, however, that the exponential gain in (3) does not typically permit timesteps of *many* round trips at once.

Next, we show how our mean-field theory leads to a NLSE with a phase potential. To do this, we ignore gain curvature; this leads to an amplitude that is constant in space everywhere but the turnaround point. Let A and ϕ be F's amplitude and phase, respectively. The derivatives in the cross-steepening term can be written as $\frac{\partial F^*}{\partial z} F = -i \frac{\partial \phi}{\partial z} |A|^2$, and the nonlinear gain simplifies to

$$g_{\mathrm{NL}} = i(\gamma_1 - \gamma_2)|A|^2 \tilde{K}\left[\frac{\partial \phi}{\partial z}\right] = -i\frac{(\gamma_1 - \gamma_2)|A|^2}{4L_c P_0}$$

$$\times \int_0^{4L_c} \frac{\partial P}{\partial z}\left(-\frac{u}{2}\right)\phi(z-u)\mathrm{d}u. \quad (4)$$

In other words, the nonlinear gain depends on the derivative of the laser's steady-state power distribution. For an asymmetric cavity with $R_1 \neq 1$ and $R_2 = 1$, we approximate the power distribution as piecewise linear. The most important feature of this curve is not the precise shape of the curve itself, but the discontinuity that occurs when the power reflects at mirror 1. (Similar results are obtained when the mirror losses are split over two mirrors.) If the change in the power at mirror 1 is denoted by ΔP, then $\frac{\partial P}{\partial z} = \frac{\Delta P}{2L_c} - \Delta P \delta(z)$, and

$$g_{\mathrm{NL}} = i(\gamma_1 - \gamma_2)\frac{|F|^2}{P_0}\frac{\Delta P}{4L_c}(\phi - \langle\phi\rangle). \quad (5)$$

After convolution, the linear part of the power profile leads to the average value of the phase, while the discontinuity at the mirror leads to its instantaneous value. Thus, *large discontinuities in power* can be considered the key ingredient for FM comb formation. After a wave has reflected, it sees a large cross-steepening term that represents its phase at a slightly earlier time. This causes the phase to experience positive feedback. Similarly, the amplitude relaxation term can be integrated to produce an equation that we refer to as the phase NLSE:

$$-i\frac{\partial F}{\partial T} = \frac{\beta}{2}\frac{\partial^2 F}{\partial z^2} + \gamma|F|^2(\phi - \langle\phi\rangle)F + ir(|F|^2 - P_0)F, \quad (6)$$

where $\gamma \equiv (\gamma_1 - \gamma_2)\frac{\Delta P}{4L_c P_0}$ is the normalized cross-steepening nonlinearity. While the phase NLSE strongly resembles the conventional intensity NLSE, there is an important difference: the intensity NLSE lacks the final term, a non-Hermitian relaxation term that attempts to force the amplitude to its steady-state value. It is this term that causes the system's dynamics to be dominated by its phase rather than its amplitude. This term is present only in active cavities with gain and discourages the formation of pulses.

By solving for the amplitude and phase separately, one can show that an analytical solution to (6) is

$$F(z, T) = A_0 \exp\left[i\frac{\gamma|A_0|^2}{2\beta}\left(z^2 - \frac{1}{3}L_c^2\gamma|A_0|^2 T\right)\right], \quad (7)$$

where $A_0 = \sqrt{P_0}(1 + \frac{\gamma}{2r})^{-1/2} \approx \sqrt{P_0}$. This is the key result, as this solution is nonperturbative and almost completely describes FM combs. It also describes higher-order harmonic states [55], which have the same mathematical form but a position that is modulo a reduced cavity length. The linear dependence of the phase on the slow time leads to a carrier–envelope offset, while the quadratic dependence on position leads to an instantaneous frequency of

$$f_i(t) = \frac{1}{2\pi}\left(\frac{c}{n}\right)^2\frac{\gamma}{\beta}|A_0|^2 t, \quad (8)$$

where we have converted from position to fast time using $t \leftrightarrow -\frac{n}{c}z$. This is a linearly chirped frequency, with a chirp rate inversely proportional to the laser's dispersion. While this simple formalism predicts that zero dispersion would produce a comb of infinite bandwidth, as we will show later, a finite gain linewidth will not allow a stable comb to exist unless the sweep bandwidth is limited.

3. DISCUSSION

First, we discuss why the frequency ends up linearly chirped. Physically, it occurred because the cross-steepening at the facet generated positive feedback on the phase, which was then mitigated by the dispersion. Mathematically, it arose because the phase evolution of the NLSE has a parabolic solution in equilibrium. When the amplitude is constant, the phase evolution is given by

$$\frac{\partial \phi}{\partial T} = -\frac{\beta}{2}\left(\frac{\partial \phi}{\partial z}\right)^2 + \gamma|A|^2(\phi - \langle\phi\rangle). \quad (9)$$

If the dispersive term is initially small, phase perturbations experience exponential gain due to the nonlinearity. If the GVD is negative, dispersion suppresses negative perturbations and enhances positive perturbations. However, at the FM turnaround point, the derivative is zero, and the exponential gain in the negative direction remains uninhibited. This generates a discontinuity in the derivative of ϕ, which leads to the production of a characteristic pulsation in the amplitude. This pulsation is physical and has been observed in several systems [6,8], but can also destabilize the comb.

Figure 3 compares the analytical results of the extendon solutions to the solutions obtained by the mean-field theory. First, we consider the case without gain curvature, shown in Fig. 3(a). The agreement between the mean-field theory and the analytic form is excellent, as the assumption of a linear intracavity power is actually a relatively weak one. The most conspicuous discrepancy is present at the turnaround point, where the assumption of a constant amplitude cannot hold, as the second derivative of ϕ is not well defined. Provided the pulsation is small, the extendon will be able to form, as spatial inhomogeneities are automatically dampened by the relaxation term. However, consider the dispersive term, whose phase evolution is given by $\frac{\partial \phi}{\partial T} = \frac{\beta}{2}(\frac{1}{A}\frac{\partial^2 A}{\partial z^2} - (\frac{\partial \phi}{\partial z})^2)$ when inhomogeneities are present in the amplitude. If the pulsation causes A to dip to near zero, the amplitude-dependent term diverges and amplitude inhomogeneities become large, destabilizing the phase. When these fluctuations are too large, they will become self-reinforcing and destabilize comb operation. In other words, these states cannot be coherent unless they extend throughout the entire cavity.

In the absence of gain curvature, there is essentially no value of the dispersion that causes the comb to destabilize—the NLSE supports infinite-bandwidth FM combs. However, once gain curvature is considered, this is no longer the case. Figure 3(b) shows the same results as in Fig. 2(a), but with gain curvature enabled. We use the same theory as before, but modify the intensity using $\delta P = -\frac{D_g}{4r}(\frac{\partial \phi}{\partial z})^2$, which is estimated by requiring that the change in amplitude due to gain curvature be balanced by the restoring force. Characteristic dips in the amplitude are now visible around the pulsation, which exist because the FM comb has deviated from its central frequency and its gain has been reduced. Thus, the power begins to fall. If the dispersion is reduced such that the FM comb bandwidth exceeds the gain bandwidth of the laser, the power will dip to near zero and the amplitude pulsation will destabilize comb operation. This leads to the following approximate condition for stable extendon formation:

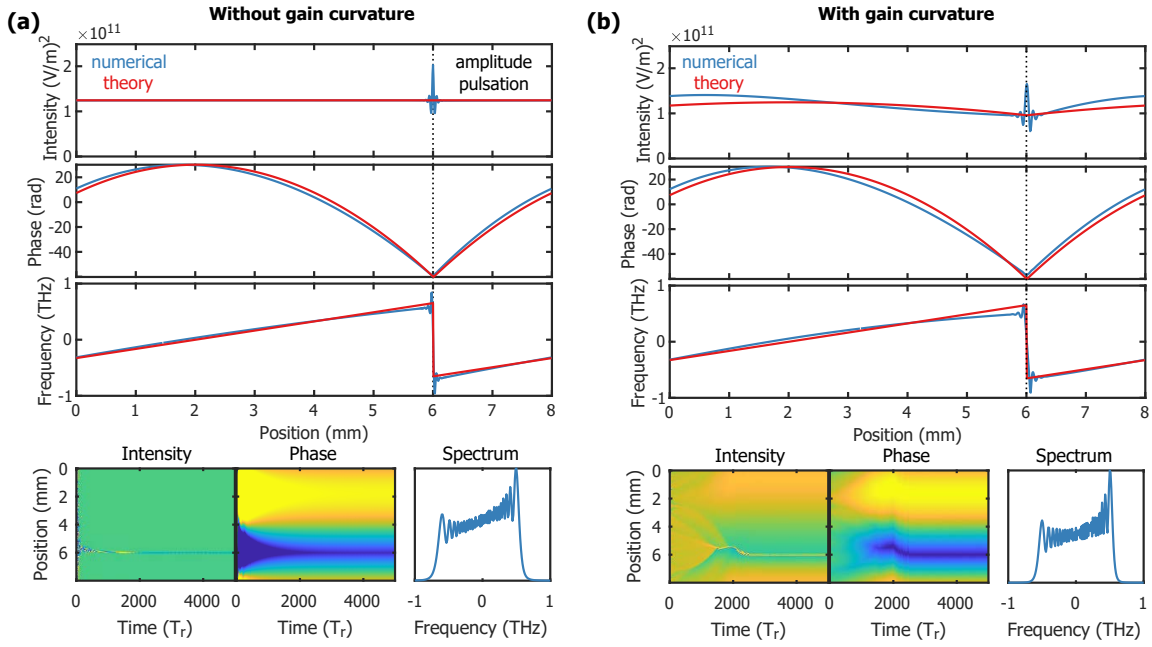

Fig. 3. (a) Comparison of mean-field simulation results and extendon theory with gain curvature disabled (GVD of $-1700\ \mathrm{fs}^2/\mathrm{mm}$ and zero Kerr nonlinearity). The agreement between the simulation and extendon theory is excellent, correctly predicting the chirp. The theory breaks down at the turnaround point, where an amplitude pulsation develops. (b) Same comparison, but with gain curvature. As the FM deviates from its center frequency, the amplitude sags due to the lower gain.

$$P_0 \frac{D_g}{4r}\left(\frac{\gamma L_c}{\beta}\right)^2 \ll 1. \tag{10}$$

Experimentally, this typically manifests as a maximum pump for which stable combs can form. As the nonlinearity is related to the gain, beyond some pump value the Risken–Nummedal–Graham–Haken instability will instead be triggered. Gain curvature also acts directly on the phase, suppressing the positive feedback. If the gain is not large enough, the laser will remain single mode. Thus, gain curvature is actually responsible for both thresholds apparent in Fig. 1(c).

These concepts also explain the formation of harmonic states in QCLs, which can be conceived of as higher-order extendons. Because the frequency cannot be stably swept by more than the gain bandwidth during a round-trip period, when the dispersion is small or the nonlinearity is large, the only stable steady-state solutions to the NLSE will have the same chirp, but with a reduced sweep bandwidth and an integer number of turnaround points. These are FM profiles that have N sweeps per round trip, and therefore sweep over only $1/N$th the bandwidth. Harmonic states are the higher-order solutions of the phase NLSE, and can also be produced within this formalism by initializing the field to be periodic at an integer harmonic of the repetition rate (Fig. 4). Since harmonic states also obey the NLSE (except at the boundaries), in terms of the fundamental solution $F_1(z, T)$, the Nth harmonic state takes the form

$$F_N(z, T) = F_1\left(z \bmod \frac{2L_c}{N}, T\right), \tag{11}$$

where the modulo operator is taken over $z \in [-\frac{L_c}{N}, \frac{L_c}{N})$. However, within this formalism, harmonic states can be only quasi-stable, as any aperiodic perturbation will eventually cause them to decay to the fundamental comb state. Defect engineering [30] effectively creates reflectors—additional sources of phase potential—that can cause harmonic states to be more stable than the fundamental extendon.

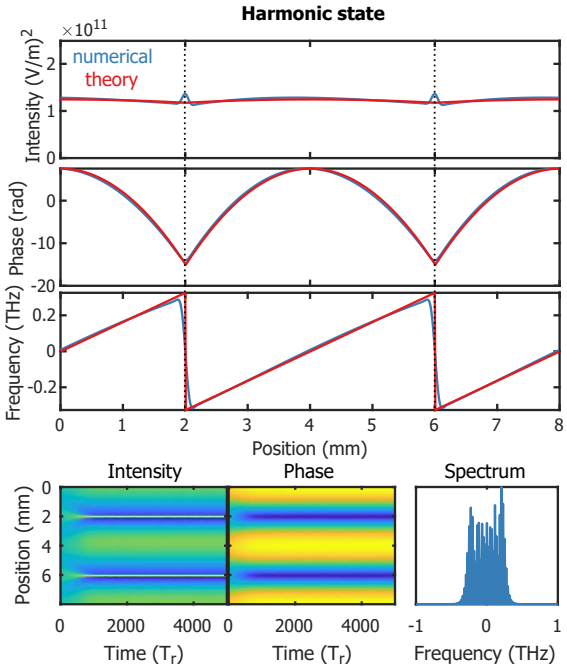

Fig. 4. Harmonic state mean-field simulation and corresponding theory (GVD of $-1700\ \mathrm{fs}^2/\mathrm{mm}$). If the field is initialized with a periodicity that is an integer multiple of the repetition rate, a harmonic comb will be produced.

While the cross-steepening nonlinearity is responsible for the creation of phase potentials and therefore FM comb formation, other optical nonlinearities can modify the extendons. For example, the Kerr nonlinearity will modify the range over which combs can be stable (see Supplement 1, Section 3). Briefly, gain curvature creates a dip in the amplitude, and the Kerr effect generates a position-dependent phase shift. As this mimics dispersion, the effective GVD is reduced by an amount proportional to the gain curvature and the Kerr nonlinearity. Conceptually, this is similar to the way in which intensity solitons have their dispersion balanced by the Kerr effect.

Which types of lasers can support broadband FM comb operation? In terms of the physical laser parameters, the total chirp over one cycle (comb bandwidth) can be calculated from Eq. (8) as

$$\Delta f = \frac{L_c}{12\pi}\alpha_m(g_0 - \alpha_w - \alpha_m)k''^{-1}(T_1 + \tfrac{1}{2}T_2), \tag{12}$$

where k'' is the physical dispersion, g_0 is the small-signal gain, α_m is the mirror loss, α_w is the waveguide loss, and T_1 and T_2 are the population and coherence lifetimes, respectively. It is interesting that this chirp depends only on a few fundamental laser parameters, which suggests that any FP laser could in principle support FM modes of operation. Although this mode of action can be suppressed by other effects, such as gain curvature and carrier diffusion, the nonlinearity comes from the gain medium itself—no saturable absorber is needed. Short gain recovery times (small T_1 values) are not needed, and in fact are actually detrimental to FM comb formation. This explains why these combs can be observed in systems such as quantum dot and quantum well lasers. Small dispersion is beneficial, but only provided the gain bandwidth is not exceeded. Small gain curvature (small T_2) is also helpful. Perhaps the most critical aspect is that the mirror losses must be large. Cross-steepening is significant only when there is a large change in the intracavity power at a facet; for $\alpha_m \approx 0$, frequency modulation is suppressed. Similarly, the mirrors must be physically adjacent to the gain medium. This explains why FM combs have tended to be observed in FP semiconductor lasers, which have a combination of large mirror losses, small gain curvatures, and large gains. Without this combination, other multimode dynamics will dominate.

4. CONCLUSION

We have shown for the first time that light in many lasers can obey a NLSE whose potential is proportional to its phase. In these systems, phase dynamics dominate due to the presence of an effective relaxation term that drives the laser to its steady-state output. The fundamental solution to this equation is a dissipative extendon with quadratic phase, a nondispersive wave whose frequency is modulated linearly in time. This explains the numerous experimental observations of FM combs in various laser systems. We arrived at this result by deriving an LLE-like mean-field theory for lasers with large internal gain, and our results explain the previously mysterious dynamics of these combs. Our results will pave the way for the development of new types of light sources utilizing these concepts, as the theory is general for many laser systems and ties together several recently discovered phenomena.

Funding. Air Force Office of Scientific Research (FA9550-20-1-0192); University of Notre Dame.

Disclosures. The author declares no conflicts of interest.

See Supplement 1 for supporting content.

REFERENCES

1. S. E. Harris and R. Targ, "FM oscillation of the He-Ne laser," Appl. Phys. Lett. **5**, 202–204 (1964).
2. A. Yariv, "Internal modulation in multimode laser oscillators," J. Appl. Phys. **36**, 388–391 (1965).
3. A. Hugi, G. Villares, S. Blaser, H. C. Liu, and J. Faist, "Mid-infrared frequency comb based on a quantum cascade laser," Nature **492**, 229–233 (2012).
4. J. B. Khurgin, Y. Dikmelik, A. Hugi, and J. Faist, "Coherent frequency combs produced by self frequency modulation in quantum cascade lasers," Appl. Phys. Lett. **104**, 081118 (2014).
5. D. Burghoff, T.-Y. Kao, N. Han, C. W. I. Chan, X. Cai, Y. Yang, D. J. Hayton, J.-R. Gao, J. L. Reno, and Q. Hu, "Terahertz laser frequency combs," Nat. Photonics **8**, 462–467 (2014).
6. M. Singleton, P. Jouy, M. Beck, and J. Faist, "Evidence of linear chirp in mid-infrared quantum cascade lasers," Optica **5**, 948–953 (2018).
7. J. Hillbrand, D. Auth, M. Piccardo, N. Opačak, E. Gornik, G. Strasser, F. Capasso, S. Breuer, and B. Schwarz, "In-phase and anti-phase synchronization in a laser frequency comb," Phys. Rev. Lett. **124**, 023901 (2020).
8. L. A. Sterczewski, C. Frez, S. Forouhar, D. Burghoff, and M. Bagheri, "Frequency-modulated diode laser frequency combs at 2 mm wavelength," APL Photon. **5**, 076111 (2020).
9. M. W. Day, M. Dong, B. C. Smith, R. C. Owen, G. C. Kerber, T. Ma, H. G. Winful, and S. T. Cundiff, "Simple single-section diode frequency combs," arXiv:2010.07062 [physics] (2020).
10. G. Villares, A. Hugi, S. Blaser, and J. Faist, "Dual-comb spectroscopy based on quantum-cascade-laser frequency combs," Nat. Commun. **5**, 5192 (2014).
11. Y. Yang, D. Burghoff, D. J. Hayton, J.-R. Gao, J. L. Reno, and Q. Hu, "Terahertz multiheterodyne spectroscopy using laser frequency combs," Optica **3**, 499–502 (2016).
12. D. Burghoff, Y. Yang, and Q. Hu, "Computational multiheterodyne spectroscopy," Sci. Adv. **2**, e1601227 (2016).
13. R. Huber, M. Wojtkowski, and J. G. Fujimoto, "Fourier domain mode locking (FDML): a new laser operating regime and applications for optical coherence tomography," Opt. Express **14**, 3225–3237 (2006).
14. A. Gordon, C. Y. Wang, L. Diehl, F. X. Kärtner, A. Belyanin, D. Bour, S. Corzine, G. Höfler, H. C. Liu, H. Schneider, T. Maier, M. Troccoli, J. Faist, and F. Capasso, "Multimode regimes in quantum cascade lasers: from coherent instabilities to spatial hole burning," Phys. Rev. A **77**, 053804 (2008).
15. D. P. Burghoff, "Broadband terahertz photonics," Ph.D. thesis (Massachusetts Institute of Technology, 2014).
16. D. Burghoff, Y. Yang, D. J. Hayton, J.-R. Gao, J. L. Reno, and Q. Hu, "Evaluating the coherence and time-domain profile of quantum cascade laser frequency combs," Opt. Express **23**, 1190–1202 (2015).
17. Z. Han, D. Ren, and D. Burghoff, "Sensitivity of SWIFT spectroscopy," Opt. Express **28**, 6002–6017 (2020).
18. F. Cappelli, L. Consolino, G. Campo, I. Galli, D. Mazzotti, A. Campa, M. S. de Cumis, P. C. Pastor, R. Eramo, M. Rösch, M. Beck, G. Scalari, J. Faist, P. D. Natale, and S. Bartalini, "Retrieval of phase relation and emission profile of quantum cascade laser frequency combs," Nat. Photonics **13**, 562–568 (2019).
19. L. Consolino, M. Nafa, F. Cappelli, K. Garrasi, F. P. Mezzapesa, L. Li, A. G. Davies, E. H. Linfield, M. S. Vitiello, P. D. Natale, and S. Bartalini, "Fully phase-stabilized quantum cascade laser frequency comb," Nat. Commun. **10**, 1–7 (2019).
20. M. Piccardo, P. Chevalier, B. Schwarz, D. Kazakov, Y. Wang, A. Belyanin, and F. Capasso, "Frequency-modulated combs obey a variational principle," Phys. Rev. Lett. **122**, 253901 (2019).
21. A. Gordon and D. Majer, "Coherent transport in semiconductor heterostructures: a phenomenological approach," Phys. Rev. B **80**, 195317 (2009).
22. Y. Wang and A. Belyanin, "Active mode-locking of mid-infrared quantum cascade lasers with short gain recovery time," Opt. Express **23**, 4173–4185 (2015).
23. C. Silvestri, L. L. Columbo, M. Brambilla, and M. Gioannini, "Coherent multi-mode dynamics in a quantum cascade laser: amplitude- and

frequency-modulated optical frequency combs," Opt. Express **28**, 23846–23861 (2020).
24. Y. Wang and A. Belyanin, "Harmonic frequency combs in quantum cascade lasers: time-domain and frequency-domain theory," Phys. Rev. A **102**, 013519 (2020).
25. P. Tzenov, D. Burghoff, Q. Hu, and C. Jirauschek, "Analysis of operating regimes of terahertz quantum cascade laser frequency combs," IEEE Trans. Terahertz Sci. Technol. **7**, 351–359 (2017).
26. M. Dong, S. T. Cundiff, and H. G. Winful, "Physics of frequency-modulated comb generation in quantum-well diode lasers," Phys. Rev. A **97**, 053822 (2018).
27. N. Henry, D. Burghoff, Y. Yang, Q. Hu, and J. B. Khurgin, "Pseudorandom dynamics of frequency combs in free-running quantum cascade lasers," Opt. Eng. **57**, 011009 (2017).
28. N. Henry, D. Burghoff, Q. Hu, and J. B. Khurgin, "Temporal characteristics of quantum cascade laser frequency modulated combs in long wave infrared and THz regions," Opt. Express **26**, 14201–14212 (2018).
29. N. Opačak and B. Schwarz, "Theory of frequency-modulated combs in lasers with spatial hole burning, dispersion, and Kerr nonlinearity," Phys. Rev. Lett. **123**, 243902 (2019).
30. M. Piccardo, B. Schwarz, D. Kazakov, M. Beiser, N. Opačak, Y. Wang, S. Jha, J. Hillbrand, M. Tamagnone, W. T. Chen, A. Y. Zhu, L. L. Columbo, A. Belyanin, and F. Capasso, "Frequency combs induced by phase turbulence," Nature **582**, 360–364 (2020).
31. F. Gustave, L. Columbo, G. Tissoni, M. Brambilla, F. Prati, B. Kelleher, B. Tykalewicz, and S. Barland, "Dissipative phase solitons in semiconductor lasers," Phys. Rev. Lett. **115**, 043902 (2015).
32. B. Meng, M. Singleton, M. Shahmohammadi, F. Kapsalidis, R. Wang, M. Beck, and J. Faist, "Mid-infrared frequency comb from a ring quantum cascade laser," Optica **7**, 162–167 (2020).
33. M. Haelterman, S. Trillo, and S. Wabnitz, "Additive-modulation-instability ring laser in the normal dispersion regime of a fiber," Opt. Lett. **17**, 745–747 (1992).
34. F. Leo, S. Coen, P. Kockaert, S.-P. Gorza, P. Emplit, and M. Haelterman, "Temporal cavity solitons in one-dimensional Kerr media as bits in an all-optical buffer," Nat. Photonics **4**, 471–476 (2010).
35. T. J. Kippenberg, A. L. Gaeta, M. Lipson, and M. L. Gorodetsky, "Dissipative Kerr solitons in optical microresonators," Science **361**, eaan8083 (2018).
36. K. Y. Yang, K. Beha, D. C. Cole, X. Yi, P. Del'Haye, H. Lee, J. Li, D. Y. Oh, S. A. Diddams, S. B. Papp, and K. J. Vahala, "Broadband dispersion-engineered microresonator on a chip," Nat. Photonics **10**, 316–320 (2016).
37. P. Del'Haye, A. Schliesser, O. Arcizet, T. Wilken, R. Holzwarth, and T. J. Kippenberg, "Optical frequency comb generation from a monolithic microresonator," Nature **450**, 1214–1217 (2007).
38. Y. Okawachi, M. R. E. Lamont, K. Luke, D. O. Carvalho, M. Yu, M. Lipson, and A. L. Gaeta, "Bandwidth shaping of microresonator-based frequency combs via dispersion engineering," Opt. Lett. **39**, 3535 (2014).
39. T. Herr, V. Brasch, J. D. Jost, C. Y. Wang, N. M. Kondratiev, M. L. Gorodetsky, and T. J. Kippenberg, "Temporal solitons in optical microresonators," Nat. Photonics **8**, 145–152 (2014).
40. T. Herr, K. Hartinger, J. Riemensberger, C. Y. Wang, E. Gavartin, R. Holzwarth, M. L. Gorodetsky, and T. J. Kippenberg, "Universal formation dynamics and noise of Kerr-frequency combs in microresonators," Nat. Photonics **6**, 480–487 (2012).
41. E. Obrzud, S. Lecomte, and T. Herr, "Temporal solitons in microresonators driven by optical pulses," Nat. Photonics **11**, 600–607 (2017).
42. D. C. Cole, A. Gatti, S. B. Papp, F. Prati, and L. Lugiato, "Theory of Kerr frequency combs in Fabry-Perot resonators," Phys. Rev. A **98**, 013831 (2018).
43. S.-P. Yu, H. Jung, T. C. Briles, K. Srinivasan, and S. B. Papp, "Photonic-crystal-reflector nanoresonators for Kerr-frequency combs," ACS Photon. **6**, 2083–2089 (2019).
44. S. Coen, H. G. Randle, T. Sylvestre, and M. Erkintalo, "Modeling of octave-spanning Kerr frequency combs using a generalized mean-field Lugiato–Lefever model," Opt. Lett. **38**, 37–39 (2013).
45. L. A. Lugiato, F. Prati, M. L. Gorodetsky, and T. J. Kippenberg, "From the Lugiato–Lefever equation to microresonator-based soliton Kerr frequency combs," Philos. Trans. R. Soc. A **376**, 20180113 (2018).
46. L. A. Lugiato and F. Prati, "Traveling wave formalism for the dynamics of optical systems in nonlinear Fabry–Perot cavities," Phys. Scr. **93**, 124001 (2018).
47. X. Xue, Y. Xuan, Y. Liu, P.-H. Wang, S. Chen, J. Wang, D. E. Leaird, M. Qi, and A. M. Weiner, "Mode-locked dark pulse Kerr combs in normal-dispersion microresonators," Nat. Photonics **9**, 594–600 (2015).
48. Y. K. Chembo and N. Yu, "Modal expansion approach to optical-frequency-comb generation with monolithic whispering-gallery-mode resonators," Phys. Rev. A **82**, 033801 (2010).
49. A. Coillet, I. Balakireva, R. Henriet, K. Saleh, L. Larger, J. M. Dudley, C. R. Menyuk, and Y. K. Chembo, "Azimuthal turing patterns, bright and dark cavity solitons in Kerr combs generated with whispering-gallery-mode resonators," IEEE Photon. J. **5**, 6100409 (2013).
50. D. C. Cole, E. S. Lamb, P. Del'Haye, S. A. Diddams, and S. B. Papp, "Soliton crystals in Kerr resonators," Nat. Photonics **11**, 671–676 (2017).
51. M. Karpov, M. H. P. Pfeiffer, H. Guo, W. Weng, J. Liu, and T. J. Kippenberg, "Dynamics of soliton crystals in optical microresonators," Nat. Phys. **15**, 1071–1077 (2019).
52. G. P. Agrawal, *Nonlinear Fiber Optics*, 5th Ed. (Academic, 2012).
53. L. A. Lugiato and F. Prati, "Self-pulsing in Fabry-Perot lasers: an analytic scenario," Phys. Rev. Res. **1**, 032029 (2019).
54. N. Henry, D. Burghoff, Q. Hu, and J. Khurgin, "Study of spatio-temporal character of frequency combs generated by quantum cascade lasers," IEEE J. Sel. Top. Quantum Electron. **25**, 1200209 (2019).
55. T. S. Mansuripur, C. Vernet, P. Chevalier, G. Aoust, B. Schwarz, F. Xie, C. Caneau, K. Lascola, C.-E. Zah, D. P. Caffey, T. Day, L. J. Missaggia, M. K. Connors, C. A. Wang, A. Belyanin, and F. Capasso, "Single-mode instability in standing-wave lasers: the quantum cascade laser as a self-pumped parametric oscillator," Phys. Rev. A **94**, 063807 (2016).
56. G. Villares, S. Riedi, J. Wolf, D. Kazakov, M. J. Süess, P. Jouy, M. Beck, and J. Faist, "Dispersion engineering of quantum cascade laser frequency combs," Optica **3**, 252–258 (2016).
57. Y. Yang, D. Burghoff, J. Reno, and Q. Hu, "Achieving comb formation over the entire lasing range of quantum cascade lasers," Opt. Lett. **42**, 3888–3891 (2017).
58. F. P. Mezzapesa, V. Pistore, K. Garrasi, L. Li, A. G. Davies, E. H. Linfield, S. Dhillon, and M. S. Vitiello, "Tunable and compact dispersion compensation of broadband THz quantum cascade laser frequency combs," Opt. Express **27**, 20231–20240 (2019).